Impact de la modélisation des protections numériques sur l'analyse probabiliste de risque pour les réseaux électriques

Impact of digital protection relay models on probability security analysis for power systems

BACH Alexandre
ULB
Bruxelles
alexandre.bach@ulb.be

HENNEAUX Pierre
ULB
Bruxelles
pierre.henneaux@ulb.be

Résumé **—** Ce papier propose une méthode d'estimation de la probabilité de défaillance cachée des relais de protection numériques des réseaux électriques de transport. Pour accompagner l'électrification croissante de l'industrie et de différents usages, il est nécessaire de garantir une fiabilité maximale du réseau électrique avec le moins de coupure de clients possible. Or, il est admis que les défaillances des systèmes de protection, dont les relais et les disjoncteurs font partie, jouent un rôle dans la cascade d'événements qui peuvent conduire à un blackout. Toutefois, les modèles de défaillances de ces relais, particulièrement ceux donnant la probabilité de mauvais déclenchements, ont été développés à partir du fonctionnement des relais électromécaniques, dont le nombre encore en service est très faible. C'est pourquoi ce papier présente une méthodologie cherchant à quantifier la probabilité de mauvais déclenchement des relais de protection numériques actuellement utilisés par les gestionnaires de réseaux. Ce papier montre que la probabilité de ce mode de défaillance n'est pas uniforme sur un réseau donné et n'augmente pas nécessairement avec le niveau de charge de la ligne protégée, contrairement à ce qui est prédit par les modèles électromécaniques.

Mots-clefs — relais de protection, défaillance cachée, déclenchement intempestif, analyse probabiliste de risque

Abstract **—** This paper proposes a framework which estimate the hidden failure probability of digital protection relays for transmission power grids. In order to support increasing electricity consumption from industries and consumers, there is a need to ensure the reliability of the power system with as little outages as possible. Besides, it has been established that failures from protection relays play a major part in cascading events that might lead to blackouts. However, failure models, and especially unwanted trip probabilities, have been built considering electromechanical relays, the type of which are being phased out and no longer produced. That is why this paper focuses on digital protective relays and tries to estimate their unwanted trip probability. It shows that this probability is neither uniform in a power system nor increase with the load level in the protected line, which contradict the models built for electromechanical relays.

Keywords — protection relays, hidden failures, unwanted trips, reliability assessment

I. Introduction and state of the art

To enable the increase electrification of industry and the rise of new usages (such as electric vehicles), the power grid should be of increasing reliability. Otherwise, the impact of outages would be increasingly damageable for the economy and the people. That is why there is a need for security assessment of power systems in order to prevent such events. Due to the very high number of uncertainties involved cascading events, the security assessment need to be probabilistic to accurately estimate the potential impact of an initiating contingency (such as the loss of a line or a bus in the grid due to the presence of a fault) [1]. Besides, static simulations (such as load-flow-based analyses) could lead to the consideration of scenarios that might not be possible when taking into account the dynamic transients of the grid and of its components (such as protection relays) [2]. That explains the need for dynamic probabilistic security assessment (PSA) for transmission grid with Monte Carlo simulations for instance [3]. However, usually only a fixed relay outage probability is taken into account when performing PSA of the grid in the literature [4].

Given that scheduled investment in grid assets might not follow the rise in electricity consumption in Europe, the power system will likely be operated closer and closer to its operational security limits in the future, meaning that a single contingency might lead to greater consequences. So, reliability of the system needs to be ensured as a failure of a protection relay, such as an unwanted trip (UT), would endanger the continuity of supply of customers [5]. Indeed, ref. [6] showed that protection relays are involved in more than three quarters of major disturbances in the US in the 1980s and ref. [5] showed the important impact of bad protection coordination on the number of outages of the customers.

There are two main types of outages for a protection system: first there is the missed trip when the relay does not send a trip signal to the circuit breaker (CB), which might result from a software or hardware failure or even from bad settings, or from a failure to operate of the CB when the trip signal is sent (the CB is stuck). Secondly, there is the unwanted trip which occurs when a relay sends a trip signal to the CB while not being needed. Security analyses should model as accurately as possible the behaviour of the protection system and use realistic values for outage probability of the protections to ensure the trustworthiness of their results. The missed trip is well studied in the literature with different methodologies describing this outage mode and estimating its frequency [7]. So, the risk derived from these outages can be easily quantified in PSA, even considering the dynamics of the electrical grid. However, this cannot be said considering the unwanted trips since the most commonly used model in the literature has been developed considering the older electromechanical relays in which the third zone timer might be stuck, leading to a relay tripping without temporization even though it should have waited for closer relays to trip first [8]. It is easily understandable that this outage mode is no longer relevant when dealing with digital relays the timer of which is digital and embedded in the processing unit.

For all these reasons, there is still a need to have a framework for estimating the UT probability of digital relays which takes into account the dynamic nature of said relays. This paper extends previous work of the authors [9] which also uses the presented software tools. The framework is detailed again and the impact of the model of the protection relay on the result of the UT probability estimation is presented. The main contribution of this paper relative to [9] is the consideration of different models of relays with different characteristics. The paper is structured as follows. Section II presents the hidden failures of protection relays and the developed methodology to estimate their frequency. Then, Section III highlights some simulations results obtained in the IEEE-14 bus test network. Finally, section IV concludes the paper and discusses future work.

II. HIDEEN FAILURE CONCEPT AND PROBABILITY ESTIMATION METHOD

A. *Limits of the current hidden failure models*

When the grid is in normal operation within security margins, an unwanted trip of a protection relay should not lead to any major disturbance (provided that the N-1 security criterion is verified) and is easily detectable by the grid operator. However, in stress conditions (following a first contingency such as the loss of one asset), the unwanted trip of a relay by sympathy can lead to the loss of more than one equipment and can potentially initiate cascading events with major consequences. Relay and CB outages during these conditions are called hidden failures. Estimating their probability of occurrence has been studied since the 1990s [6]. Even though missed trips are well documented, there is no model from which deriving the UT probability of a digital relay, which is the motivation for the paper.

Besides, some PSAs are based on quasi-static computations (load flow solutions) or sometimes root mean square (RMS) balanced phasors (such as the Dynawo software tool [10]) which do not represent the transient variations of the signals measured by the relays, especially at the inception time of a fault or at the opening time of a CB. Given that the most common type of fault is single-phase-to-line fault (around 80% of the encountered cases) and given that a balanced solver cannot simulate such type of fault, we can say that using a solver able to compute electromagnetic transients (EMTs) is needed to model the transient response of relays and take into account the computations which are performed at each time step. That is why, a framework able to evaluate the impact of single-phase faults with EMT simulations is relevant to model relay coordination.

B. *Dynamic modeling of the grid and the protection system*

As stated, the proposed framework is able to perform time domain simulations with digital relay models to estimate the UT probability considering different parameters variations. To have an easily programmable and automatic tool, this paper uses MATLAB/Simulink with its specialized power systems library as base software tool to perform the EMT unbalanced simulations of power systems (in normal and fault conditions). This framework is flexible as it is possible to programmatically build power grid models from the line impedance data and the generation and/or consumption at each node. So, for a given grid topology, the framework builds an electrical model with lines, transformers, generators and loads. Then, EMT simulations are performed and the electrical measurements at each relay position (for instance at each end of all the lines) are stored.

C. *UT probability estimation*

Once the electrical signals at each relay locations have been simulated for each time step of the considered event sequence, the second step of the framework is the simulation of the protective relays. Since it is known that only the relays which are located close enough to the initiating event have a non-negligible probability of UT, a region of vulnerability (RV) is defined around the simulated initiating contingency. The RV is defined as composed of all relays being distant of less than a given value of the simulated event. For example, if we consider the grid in Fig. 1 and a fault on line $1 \leftrightarrow 2$. Then, the relays at the two ends of said line (i.e. R_{21} & R_{12}, with R_{ij} the relay at node i protecting the line $i \leftrightarrow j$) are located in the RV of distance 1. We can note that with this definition, the relays in the RV of distance 1 are the ones supposed to trip first to isolate the fault in the smallest area possible. If we were to consider a RV of distance 2, then the relays ($R_{12}, R_{21}, R_{15}, R_{51}, R_{25}, R_{52}, R_{23}, R_{32}, R_{24}, R_{42}, R_{45}, R_{54}$) would need to be taken into account and their behaviour simulated at each time step of the simulation. Defining such RV increase the simulation speed of the framework, and by such enables us to consider more parameters variations, while almost not decreasing at all the estimated risk as it is admitted that only close enough relays are subject to sympathetic unwanted tripping when a fault occurs at a given location on a given grid.

For each relay in the RV, its trip signals are computed given the chosen relay characteristics and settings. Having the trip time of every relay in the RV and considering the PDF of the CB opening time, it is possible to compute the probability of a distant relay (a relay being in the RV of distance $k > 1$ while not being part of the RV of distance 1) to trip faster than one of the closest relays (in the RV of distance 1). Let r be the opening time of the slowest of the two closest CBs in the RV of distance 1 (which should both open first before any other CB), and let r' be the opening time of one of the CB inside the considered RV, then the conditional probability of UT knowing that there is a fault (event F), noted $\mathbb{P}(UT|F)$, can be computed according to (1):

$$\mathbb{P}(UT|F) = \mathbb{P}(r' \leq r) \tag{1}$$

We chose to present the values of the conditional probability of UT knowing the presence of a fault because it is this value that would be used to conduct PSA in cascading outages of power systems. The algorithm is summarized in the flowchart in Fig. 2.

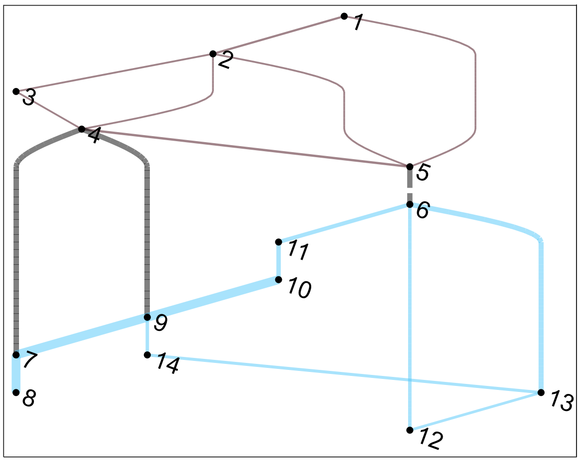

Fig. 1. The IEEE 14-bus test network with the 69 kV lines represented in red and the 13.8 kV ones in blue. The widths of the lines are proportional to their lineic conductance. The power transformers are represented by black lines between two voltage levels.

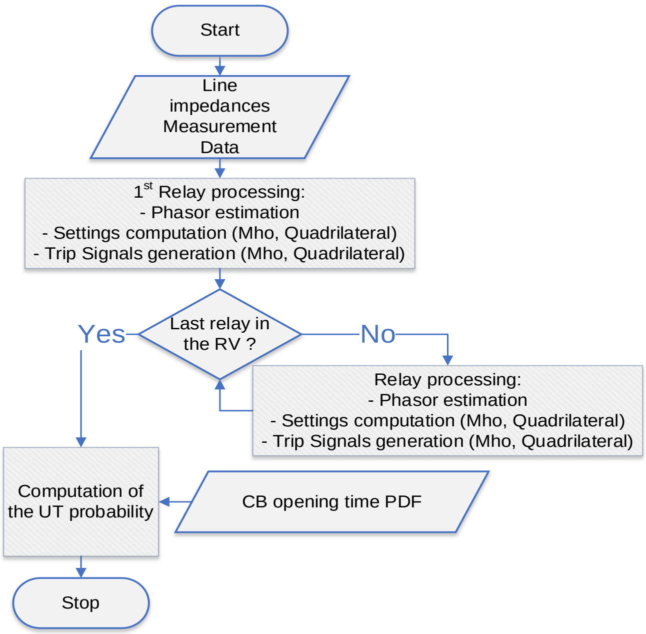

Fig. 2. Algorithm flowchart for UT probability estimation from the different electrical simulations.

III. Results

A. *Use case*

In this paper, the presented results have been obtained applying the methodology on a single benchmark grid: the IEEE-14 node benchmark grid as described in [11]. The generators are modelled as a constant voltage source in series with a transient impedance with a grounding impedance $Z_{nG} = 25\ \Omega$ [12]. The model used for loads is constant delta-coupled impedances. The lines are described with a PI lumped-parameters models. The power transformers are considered being three phases 2 windings DY coupled with a neutral grounding impedance $Z_{nT} = 40\ \Omega$ [12]. The topology of the grid is presented in Fig. 1.

Usually, PSA consider three-phase metallic faults since they lead to the highest short-circuit current possible. This approach could be seen as a conservative one given that if the grid is able to withstand such currents, it should be able to cope with faults generating lower currents. However, three-phase metallic faults are the easiest to detect (since they generate such high currents), meaning that the probability of a missed or unwanted trip of a relay can be lower with well-chosen settings. That is why we proposed to consider only single-phase faults to the ground (A-G faults) in this paper since they are not usually considered while being the most common and still being challenging for the protection scheme. The fault rate is considered uniformly distributed on the lines with $\mathbb{P}_F = 0.27\ fault/100km$ [3]. We consider only the relays protecting the lines with a relay present at both ends of each one of them. In our experiments, the 17 lines are tested as potential faulty lines with probability $\mathbb{P}_F . L_{lig}$, L_{lig} being the length of the line. For each faulty line, the design of experiment considers 5 parameters with uniform PDF across their possible values:

- The fault inception angle, with $[0, 90, 180]°$ considered.
- The location of the fault on the line $m \in [0.1, 0.5, 0.9]$ with respective probabilities of occurring $\mathbb{P}_F . L_{lig} . [0.3, 0.4, 0.3]$
- The fault resistance value $R_f \in [0.001, 0.1, 1, 10]\ \Omega$.
- The load level multiplier $Load_{lvl} \in [0.5, 1, 1.5]$ with respect to the nominal load level found in the database [11].

- The relay characteristic with one residual overcurrent and 3 distance elements considered (Mho and 2 quadrilaterals with different resistive reach).

So, the design of experiment has led to $17 \times 108 = 1{,}836$ electric fault simulations (not counting the relay characteristics). For each electrical simulation, all relays within the Region of Vulnerability of distance 2 are simulated and the trip signals for the overcurrent and the three distance elements are stored in the database.

B. *Relay models*

The relays are modelled as using the estimated fundamental phasors of the measured current and voltage to operate. We can see in Fig. 3 the measured phase voltage and current at relay R_{12} (close to node 1 on the line $1 \leftrightarrow 2$) given a fault occurring at distance $m = 10\%$ of the said line at instant $t_f = 0.5\ s$. It appears that this simulation tool provides us with realistic time-domain evolutions of the signals. We can also see the evolution of the magnitude of the estimated phasor using DFT.

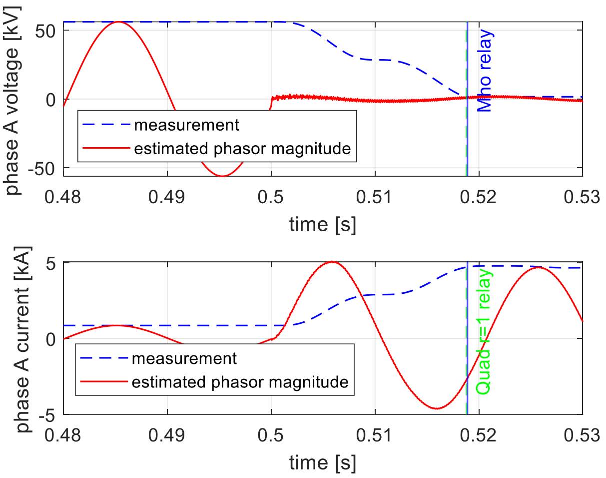

Fig. 3. Phase voltage and current measured at relay R_{12} with an AG fault of resistance $R_f = 0.001\ \Omega$ at $m = 10\%$ of the line $1 \leftrightarrow 2$ occuring at $t_f = 0.5\ s$. The estimated trip times of the Mho characteristic relay (blue) and of the quadrilateral characteristic one with $r = 1$ (dashed green) are shown with vertical lines.

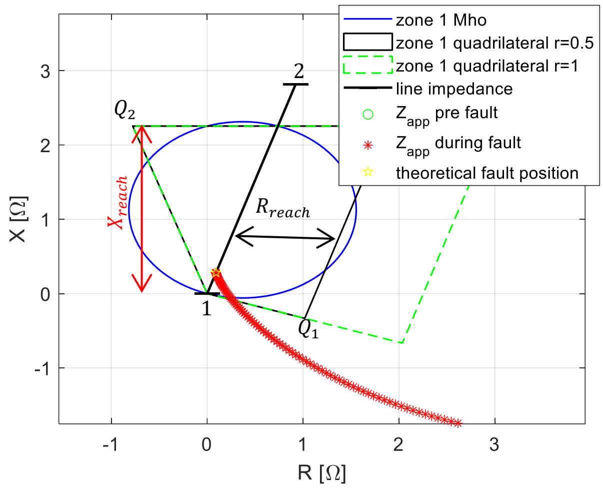

Fig. 4. Apparent impedance locus and first zone of the three considered relay characteristic for the considered fault of Fig. 3.

Two types of protection relays for the lines are being tested in parallel (concomitant use): a distance relay and a residual overcurrent relay. The settings of the relays are chosen accordingly to [13]. For each line of positive sequence impedance Z_{lig}, of zero sequence impedance Z_{0lig} and of nominal current value I_n, the residual overcurrent relay is composed of an extremely inverse characteristic with pickup current $I_P = 0.12 \times I_n$ and of an instantaneous trip signal which is sent when the residual current is greater than I_n. Regarding the choice of the distant element, three characteristics are studied in this paper: First, a Mho distance relay computes at each time step the apparent impedance and the estimated fault distance according to (2).

$$\begin{cases} Z_{app} = \dfrac{V_A}{I_A + 3.K_0 I_0} \\ \hat{m} = \dfrac{Z_{app}.Z_{app}^*}{\Re\left(Z_{lig}.Z_{app}^*\right)} \end{cases} \tag{2}$$

With $K_0 = \frac{Z_{0lig} - Z_{lig}}{3.Z_{lig}}$, with V_A being the phasor of the phase A voltage estimated using DFT, with I_A being the phase A current phasor and with I_0 being the zero-sequence current phasor. The first zone trip signal is being sent to the CB when $\hat{m} \in [0, 0.8]$ and the second zone trip signal when $\hat{m} \in [0.8, 1.2]$, as usually done in real power systems.

Secondly, the two quadrilateral distance elements compare the apparent impedance to 4 binders. The resistive reach binder X_{reach} is chosen equal to $0.8 \times X_{lig}$ for the first zone and $1.2 \times X_{lig}$ for the second zone respectively, which is the same as for the Mho distance element. The right resistive binder is chosen proportional to the reactive reach and parallel to the line impedance, i.e. $R_{reach} = rX_{reach}$ with $r \in \{0.5, 1\}$ in this paper. $r = 0.5$ correspond to a characteristic similar to a Mho element while $r = 1$ should enable to detect more easily high resistance faults. Then, the last two point needed to define a quadrilateral element are chosen to verify (3):

$$\begin{cases} \angle\overrightarrow{1Q_1} = \angle\overrightarrow{12} - \dfrac{\pi}{2} \\ \angle\overrightarrow{1Q_2} = \alpha = 110° \end{cases} \tag{3}$$

With $\angle\vec{A}$ the angle of $\vec{A}$. With $1 = (0,0)$. Fig. 4 shows the locus of the apparent impedance Z_{app} computed from the relay according to (2) and shows the three distance elements of relay R_{12}. As expected, Z_{app} converges to $m.Z_{lig}$ and enter the three distance characteristics, meaning that the three different elements will trip. However, as Z_{app} enter the characteristics from the down part, the trip time is not different by a large factor since the three characteristics are close to each other on that part. This can be seen in Fig. 3 where the trip time of the Mho relay ($t_{trip}^{Mho} = 0.5189s$) and the one of the large quadrilateral relay ($t_{trip}^{quad=1} = 0.5188s$) are shown. We would have observed a larger difference in trip times provided that Z_{app} would have enter the protected zone from the right to the left where the characteristics are very different.

C. *Reliability assessment*

Knowing the time at which each relay will send a trip signal to its CB, the time that will take the CB to open the line is needed to evaluation the conditional probability $\mathbb{P}(UT|F)$. This time t_{CB} is random as it depends on the inception time of the fault, on the aging of CB and many other parameters. In this paper, we used a uniformly distributed $t_{CB} \in [0.08 \pm \Delta CB]s$ with $\Delta CB = 0.01s$ which is close to the values present in the literature. Provided that the opening time of two different breakers are two independent events, it is possible to compute the UT probability defined in (1) with (4):

$$\mathbb{P}(UT|F) = \mathbb{P}(r' \leq r) = \int_{r-\Delta CB}^{r+\Delta CB} \frac{F_{R'}(t)dt}{2.\Delta CB} \quad (4)$$

$F_{R'}(t) = \mathbb{P}(r' \leq t)$ being the CDF of r'. For instance, if the trip time of the slowest relay in the RV of distance 1 is $0.51s$ while another relay sends a trip signal a time $0.515s$, then the probability of the other relay opening before the closest one is $\mathbb{P}_{UT|F} = 0.2822$. We understand that the CB plays an important role in the computation of the UT probability as in this example the closest relay is quicker than the farthest away but still there is a large probability of the farthest CB opening before the closest one due to the relatively large value of ΔCB. Across all experiments (for the different fault positions, fault resistance, fault inception angle), the unwanted triggering probabilities have been computed and averaged (considering that the inception angle and resistance value are uniformly distributed and considering the probability of multiple faults occurring at the same time being negligeable) in order to compare the 34 different relay locations in terms of risk. Fig. 5 shows the conditional UT probability for all relays with a considered Mho distance element while Fig. 6 shows the difference between the UT probability considering the largest quadrilateral distance element and the one computed using a Mho element.

From the gathered averaged results, it can be said that the unwanted outage rate is not at all uniformly distributed across the grid. Indeed, there is a factor of about 100 between the relay with the highest UT probability (11.2%) and the ones with the lowest one (0.14%). This factor means that models that describes the UT probability as a fixed value applied to all relays in a network might not led to plausible results in term of risk assessment. Indeed, the medium voltage (MV, blue in Fig. 1) relays are far less likely to unwanted trips than the ones at the high voltage (HV, red in Fig. 1) level (except for the lines between nodes 6 and 9 of medium UT probability). Since the mechanical third zone timer being stuck does not apply anymore, operators should investigate other origin for sympathetic tripping. Moreover, the shape of the characteristic does not seem to play an important role in the value of the UT probability as the values obtained for the three distant elements are close from each other. As for the UT probability value, it appears that the impact of the choice of the distance element is not uniform across the grid as there are some relays which present a lower UT probability with quadrilateral elements, yet some are more likely to sympathetic tripping using such element instead of the Mho shape. Besides, the most loaded nodes are the nodes 2,3 and 4 and we can see that the relays protecting this area present the highest UT probability.

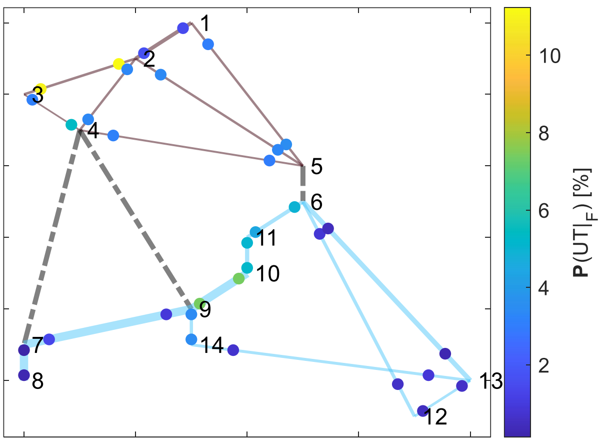

Fig. 5. Average UT probability across all the relays considering a Mho distance element.

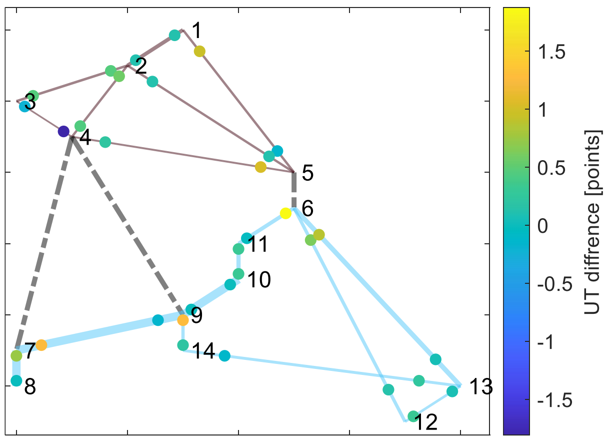

Fig. 6. Difference in UT probability between the use of a Mho distance element and a quadrilateral ($r = 1$) distance element.

That is why we studied more precisely the impact of the load level on the value of $\mathbb{P}(UT|F)$. Fig. 7 shows the repartition of the UT probability for two of the three considered load levels and compare the Mho relay with the largest quadrilateral one. In the case of low load level ($Load_{lvl} = 0.5$) the average UT probability of Mho relays is 3.07% while being of 3.28% for the large quadrilateral. This is explained by the fact that the characteristic being larger, there is naturally a larger probability of the quadrilateral relay to pick-up for distant faults. When the load level in increase to 150% of its nominal value, the UT probabilities are increased to reach respectively 3.40% and 3.74% for the two types of distance relays. If we sort the relays by the current flowing in their protected line before fault, as in Fig. 8, we can observe that there is no clear correlation between the load current and the value of the unwanted trip probability. However, this is usually supposed in the literature, as in Fig.1. of ref. [2]. We can even see that the relays present at the HV level (represented with a star in Fig. 8) show a rather flat evolution of the UT frequency with respect to the value of the load current, in total contradiction with the current models. This might result from the UT probability depending more on the value of the current during fault conditions rather than before the fault inception. To summarize, we can say that the first results from our framework tend to invalidate any model with uniform probability of sympathetic tripping of a relay in the vicinity of a fault.

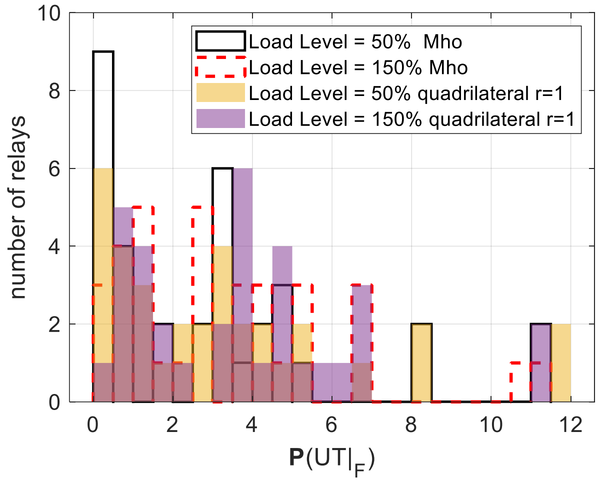

Fig. 7. Repartition of the UT probability across the 34 relays.

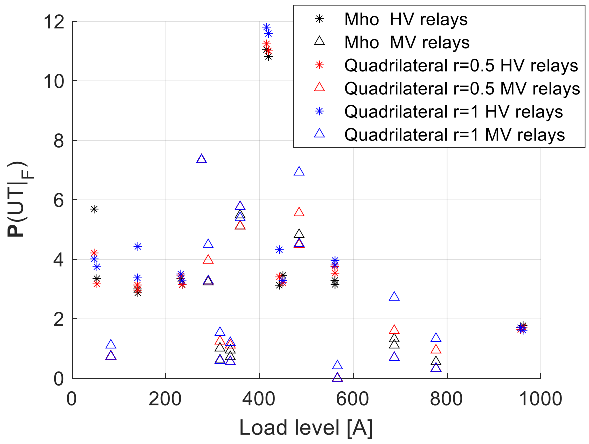

Fig. 8. Average UT probability on all relays in function of the load current before fault.

Then, we studied the impact of the fault resistance value on the UT probability as this parameter is not usually considered (since most of the literature deals with metallic faults). In Fig. 9, we can see that the UT probability of Mho relays and the smallest quadrilateral ones are similar, which is logical since their shape is similar. Yet, the large quadrilateral relays tend to have a higher UT probability than the other 2, as observed with the load level. We can see that the UT probability decreases quickly with the fault resistance, which does not mean that the protection system is more reliable but rather that most relays do not detect the presence of the fault anymore when the fault resistance is too high. So, we see a decrease in the UT probability, but we would see an important increase in missed trip probability too, which is not in the scope of this paper. For metallic fault (the considered fault resistance is $10^{-3}\Omega$) the UT probability is 5.54% for Mho relays while being of 6.03% for quadrilateral relays. These values drop dramatically for a low ohmic fault with a 10 Ω resistance to respectively 0.6% and 0.72% as the fault no longer appears neither in the zone 1 or zone 2 of the distance element nor generate a high enough residual current to trigger the instantaneous overcurrent protection (the inverse time one being very not likely to trip before the first zone of the closest relays).

For each line, we tested three fault positions at 10%, 50% and 90% of the line. Fig. 10 shows the evolution of $\mathbb{P}(UT|F)$ with respect to this parameter for the three considered distance relay types. As for the two other studied parameters, the difference between the three relay types is limited to around 10% in UT probability: between 3.03% for Mho relays and 3.39% for large quadrilateral ones for faults at distance $m = 50\%$ of the lines for instance. It seems that the faults located around the middle of the lines are the ones which are less likely lead to hidden outages of the protection. This comes from the fact that the two close-in considered faults (at 10% and 90% of the lines) are located outside of the first zone of the relays since we chose the reactive reach of this zone to be 80%. This slows down their expected time to send a trip signal to the CB as they need to wait for the second zone temporization or the time inverse overcurrent one, which naturally increases the likelihood of another relay tripping first. The asymmetry that is shown results from the choice of origin of the lines for the HV ones, with the most loaded node of being the second extremity (so being considered at 90% rather than 10% of the line).

In our simulations, the impact from the inception time, and by such the inception angle, is the smallest of all studied parameters. Indeed, in average the UT probability of a Mho relay varies from 2.69% to 3.48% and the one of a large quadrilateral relay varies from 2.78% to 3.90%. The maximum and minimum values however do not present any significant variations. This might result from the low-pass filter effect of the fundamental phasors estimation using the Fourier transform, which tend to mitigate large transient effects that could appear when the fault occurs while the instantaneous voltage is ats its peak value.

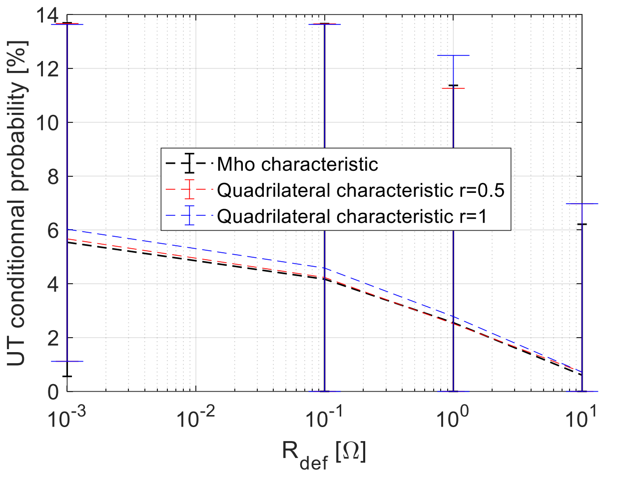

Fig. 9. Evolution of the UT probability in function of the fault resistance value. The average values are represented by the lines while the minimum and maximum values are represented with the error bars.

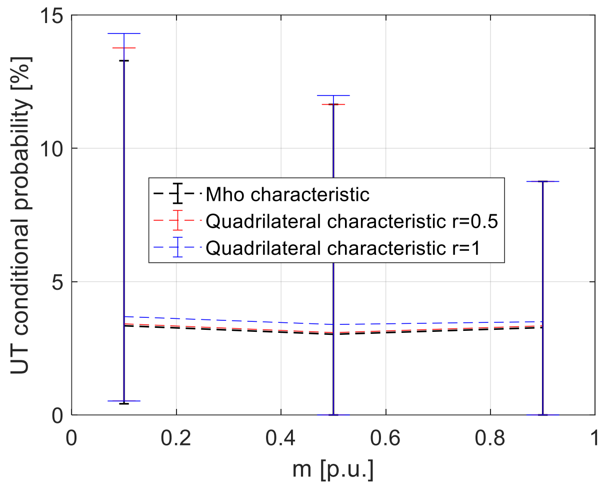

Fig. 10. Evolution of the UT probability in function of the fault distance m. The average values are represented by the lines while the minimum and maximum values are represented with the error bars.

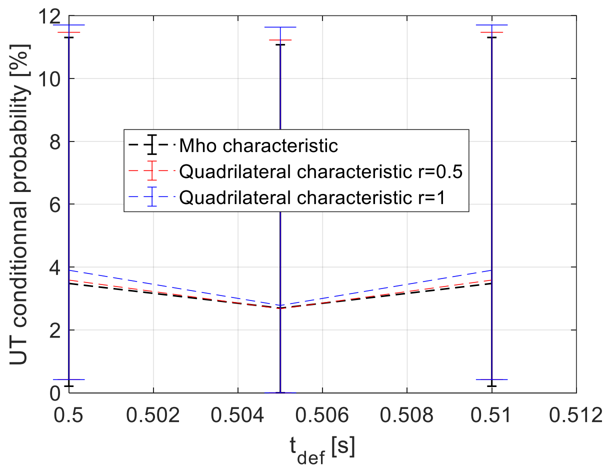

Fig. 11. Evolution of the UT probability in function of the fault inception time. The average values are represented by the lines while the minimum and maximum values are represented with the error bars.

IV. CONCLUSION AND PERSPECTIVES

To concludes, this paper presents a framework which enable the estimation of the hidden outage probability of the protection devices for transmission grids. This paper focuses on unwanted trips as they are less dealt with in the literature. We can say that the average values estimated for UT probabilities are close to the ones usually used and derived from older models. Indeed, for a fault with a resistance strictly inferior to 1 Ω (where the distance relays are working well), the estimated average UT probability is around $\mathbb{P}(UT|F) \approx 0.05$. This value is in the same order of magnitude as the values found in the literature, for instance ref. [8] used the value 0.04 while ref. [14] also used 0.05.

Then, this methodology, based on EMT simulations can be said to deliver coherent results regarding hidden outages frequency. It enables the operator to conduct a priori investigations regarding the nodes with higher risk and regarding the parameters that affect the outage probability the most. The results presented in this paper focus on the fault position, resistance value and inception time as well as the shape of distance elements. Our study shows that UT probability is linked to the load level in the vicinity of the relay and can vary by a factor of 100 in the same power systems. That is why models based on the third zone timer being stuck (with usually a constant probability across the grid) cannot model accurately the behaviour of digital relays. Instead, there is a need to dynamically simulate these trip signals (using a Monte-Carlo random sampling for instance) in order to better understand the cascading events. This study shows that the type of distance element (Mho, quadrilateral) has a rather limited influence on the hidden outage probability, with a variation of about 10%. However, as for the UT probability itself, this variation appears not to be uniform across a power system.

Further work should apply this framework on a more complex and more densely meshed grid, as well as consider uncertainty and potential errors sources such as uncertainty on the line impedance parameters (which are not well known, especially in zero-sequence) or measurement errors coming from the current and voltage transformers. Besides, more realistic models of generators including their governor speed regulating unit and of the loads with dynamic variations with respect to the voltage magnitude and frequency need to be implemented in order to verify that the presented results are still valid considering more realistic power grid dynamics. Moreover, the EMT simulations should include the simulation of the first CB opening and quantify the evolution of the UT probabilities after this event in order to propose a dynamic value of the hidden outage probabilities. Finally, other types of relays should be investigated, such as high speed relays which use the time-domain signals instead of the estimated phasors, as we can think that these relays would be much more sensitive to the inception time of the fault and less sensitive to other parameters.

ACKNOWLEDGEMENT

This work has been prepared with the support of the Belgian Energy Transition Fund, project CYPRESS (https://cypress-project.be).

REFERENCES

[1] P. Henneaux, J. Song, and E. Cotilla-Sanchez, "Dynamic probabilistic risk assessment of cascading outages," in *2015 IEEE Power & Energy Society General Meeting*, Denver, CO, USA: IEEE, Jul. 2015, pp. 1–5. doi: 10.1109/PESGM.2015.7286024.

[2] E. Ciapessoni, D. Cirio, and A. Pitto, "Cascadings in large power systems: Benchmarking static vs. time domain simulation," in *2014 IEEE PES General Meeting | Conference & Exposition*, Jul. 2014, pp. 1–5. doi: 10.1109/PESGM.2014.6939469.

[3] F. Sabot, P. Henneaux, and P.-E. Labeau, "MCDET as a Tool for Probabilistic Dynamic Security Assessment of Transmission Systems," in *2021 IEEE Madrid PowerTech*, Madrid, Spain: IEEE, Jun. 2021, pp. 1–6. doi: 10.1109/PowerTech46648.2021.9494758.

[4] H. Kameda and K. Yamashita, "RELIABILITY ANALYSIS FOR PROTECTION RELAYS," 2008.

[5] I. G. N. S. Hernanda, E. N. Kartinisari, D. A. Asfani, and D. Fahmi, "Analysis of protection failure effect and relay coordination on reliability index," in *2014 The 1st International Conference on Information Technology, Computer, and Electrical Engineering*, Semarang, Indonesia: IEEE, Nov. 2014, pp. 366–371. doi: 10.1109/ICITACEE.2014.7065773.

[6] A. G. Phadke and J. S. Thorp, "Expose hidden failures to prevent cascading outages [in power systems]," *IEEE Comput. Appl. Power*, vol. 9, no. 3, pp. 20–23, Jul. 1996, doi: 10.1109/67.526849.

[7] M. Zeynivand and S. M. Shahrtash, "Direct identification of Multi-Hidden failures in main distance relays of transmission systems," *Int. J. Electr. Power Energy Syst.*, vol. 146, p. 108722, Mar. 2023, doi: 10.1016/j.ijepes.2022.108722.

[8] D. P. Nedic, "Simulation Of Large System Disturbances," phdthesis, University of Manchester Institute of Science and Technology, 2003. [Online]. Available: https://www2.ee.washington.edu/research/real/Library/Thesis/Dusko_NEDIC.pdf

[9] A. Bach and P. Henneaux, "Unwanted trip probability estimation of digital protection relays using time-domain simulations," accepted for presentation at the 18th International Conference on Probabilistic Methods Applied to Power Systems (PMAPS 2024), Jun. 2024.

[10] A. Guironnet, M. Saugier, S. Petitrenaud, F. Xavier, and P. Panciatici, "Towards an Open-Source Solution using Modelica for Time-Domain Simulation of Power Systems," in *2018 IEEE PES Innovative Smart Grid Technologies Conference Europe (ISGT-Europe)*, Oct. 2018, pp. 1–6. doi: 10.1109/ISGTEurope.2018.8571872.

[11] "IEEE 14-Bus System - Illinois Center for a Smarter Electric Grid (ICSEG)." Accessed: Feb. 12, 2024. [Online]. Available: https://icseg.iti.illinois.edu/ieee-14-bus-system/

[12] J.-L. Chanelière, "Protection des réseaux de transport et de répartition contre les courts- circuits et les défauts d'isolement," *Réseaux Électr. Appl.*, Nov. 2009, doi: 10.51257/a-v1-d4801.

[13] B. Kasztenny, "Settings Considerations for Distance Elements in Line Protection Applications," in *2021 Texas A&M Conference for Protective Relay Engineers*, Mar. 2021.

[14] D. Pal, B. Mallikarjuna, M. Jaya Bharata Reddy, and D. K. Mohanta, "Analysis and Modeling of Protection System Hidden Failures and Its Impact on Power System Cascading Events," *J. Control Autom. Electr. Syst.*, vol. 30, no. 2, pp. 277–291, Apr. 2019, doi: 10.1007/s40313-019-00444-3.